Role of quantum coherence in shaping the line shape of an exciton interacting with a spatially and temporally correlated bath

Rajesh Dutta, Kaushik Bagchi, and Biman Bagchi

Citation: The Journal of Chemical Physics **146**, 194902 (2017); doi: 10.1063/1.4983223
View online: http://dx.doi.org/10.1063/1.4983223
View Table of Contents: http://aip.scitation.org/toc/jcp/146/19
Published by the American Institute of Physics

Role of quantum coherence in shaping the line shape of an exciton interacting with a spatially and temporally correlated bath

Rajesh Dutta,[1] Kaushik Bagchi,[2] and Biman Bagchi[1,a)]
[1]*SSCU, Indian Institute of Science, Bangalore 560012, India*
[2]*Department of Mathematics, Ohio State University, Columbus, Ohio 43210, USA*

(Received 23 January 2017; accepted 26 April 2017; published online 15 May 2017)

Kubo's fluctuation theory of line shape forms the backbone of our understanding of optical and vibrational line shapes, through such concepts as static heterogeneity and motional narrowing. However, the theory does not properly address the effects of quantum coherences on optical line shape, especially in extended systems where a large number of eigenstates are present. In this work, we study the line shape of an exciton in a one-dimensional lattice consisting of regularly placed and equally separated optical two level systems. We consider both linear array and cyclic ring systems of different sizes. Detailed *analytical calculations* of line shape have been carried out by using Kubo's stochastic Liouville equation (SLE). We make use of the observation that in the site representation, the Hamiltonian of our system with constant off-diagonal coupling J is a tridiagonal Toeplitz matrix (TDTM) whose eigenvalues and eigenfunctions are known analytically. This identification is particularly useful for long chains where the eigenvalues of TDTM help understanding crossover between static and fast modulation limits. We summarize the new results as follows. (i) In the slow modulation limit when the bath correlation time is large, the effects of spatial correlation are not negligible. Here the line shape is broadened and the number of peaks increases beyond the ones obtained from TDTM (constant off-diagonal coupling element J and no fluctuation). (ii) However, in the fast modulation limit when the bath correlation time is small, the spatial correlation is less important. In this limit, the line shape shows motional narrowing with peaks at the values predicted by TDTM (constant J and no fluctuation). (iii) Importantly, we find that the line shape can capture that quantum coherence affects in the two limits differently. (iv) In addition to linear chains of two level systems, we also consider a cyclic tetramer. The cyclic polymers can be designed for experimental verification. (v) We also build a connection between line shape and population transfer dynamics. In the fast modulation limit, both the line shape and the population relaxation, for both correlated and uncorrelated bath, show similar behavior. However, in slow modulation limit, they show profoundly different behavior. (vi) This study explains the unique role of the rate of fluctuation (inverse of the bath correlation time) in the sustenance and propagation of coherence. We also examine the effects of off-diagonal fluctuation in spectral line shape. Finally, we use Tanimura-Kubo formalism to derive a set of coupled equations to include temperature effects (partly neglected in the SLE employed here) and effects of vibrational mode in energy transfer dynamics. *Published by AIP Publishing.* [http://dx.doi.org/10.1063/1.4983223]

I. INTRODUCTION

Recent years have seen an enormous growth of interest in the energy transfer processes in photosynthetic systems[1,2] and in conjugated polymers.[3–7] In addition to these important systems, the study of excitonic energy transfer in molecular crystals has been a subject of long and sustained interest. Experimentally one studies not only energy transfer dynamics but also optical line shapes in these systems. Line shape is one of the most important tools by which we study dynamics in correlated systems and thereby understand the role of the different factors in a given energy transfer process. However, most of the theoretical studies of coherence have been limited to molecular systems, like studies of electronic and vibrational coherence in molecules and dimers. That is, extended systems have not been studied adequately in the past. Recent pioneering works by Fleming and co-workers have given impetus to the latter problem.[1]

Several recent studies have been devoted to the efficiency of energy transfer in photosynthetic and model dimer systems.[8–15] In a recent work, Moix, Khasin, and Cao[16] have studied the effect of static disorder and dephasing in diffusion of exciton and line shape concluding that with increase of the dephasing rate, line shape becomes Lorentzian (as may be expected). However, in the opposite limit, i.e., in the limit of small dephasing rate, the line shape is Gaussian. In an extended correlated system, coherence is propagated and promoted by the presence of a significant time independent off-diagonal coupling between different spatially separated groups or sites. Here coherence takes a somewhat different shape than what we encounter in energy relaxation in an isolated molecular systems where coherence is discussed among, say, different vibrational energy levels.[17–21] The situation is even more

a)Email: profbiman@gmail.com

complicated in an extended quantum system in the presence of dynamical disorder.[22] As far we are aware, there is yet no systematic study of these two factors on the coherence and line shape even in two level dimeric systems. Most of the studies employ quantum master equation formalism which has certain limitations. First, one needs to employ perturbative expansion and truncation (mostly after 2nd order) which is not appropriate for photosynthetic systems. Second, approach is often Markovian. Third, it is difficult to take into account spatial correlations which could be important in a correlated system. To mimic these types of systems and to avoid such kind of approximations, one may require a theory which is more rigorous.

There are certain lacunae even in the established studies. A connection between population transfer dynamics that easily reflects the presence of coherences through oscillatory time dependence and the optically measured line shapes has not been explored. Also, detailed analysis of the propagation of coherences (off-diagonal elements) in both slow and fast modulation limit has also not been performed. Furthermore, line shape behavior during crossover from slow to fast modulation limit, i.e., intermediate regime has not been examined yet.

Experimentally first Zewail and Harris[23–25] and subsequently Fayer and Harris[26,27] observed the presence of quantum coherence in early eighties. Haken *et al.*[28–30] and independently Silbey and Yarkony[31,32] calculated absorption line shape in the presence of exciton transfer in dimer. Their study was limited to the case where the line shape was Lorentzian. Later Sumi[33] explained Gaussian and Lorentzian behavior of the line shape in strong scattering and weak scattering limit. Silbey and Jackson[34] further investigated the exciton transfer line shape which mainly highlighted Sumi's observation. The main limitation of these studies was the restriction of the Markov process. Scholes *et al.*[35,36] experimentally detected splitting of absorption band of dimer naphthalene though the absorption bands were not symmetric due to the contribution of vibration. Jang and Silbey[37] assumed quasi-static disorder and calculated line shape for a model dimer and B850 ring of LH2 photosynthetic complex using quantum master equation based formalism. Schröder *et al.*[38] considered static disorder and compared line shape of B850 ring of LH2 using several Markovian and approximated non-Markovian formalisms in the cases of short, medium, and long bath correlation time. Most of the above studies employed either Markovian approximation or approximated non-Markovian theories and dynamic disorder was not considered completely. Few years ago, Donehue *et al.*[39] studied cyclic thiophene oligomers of 12, 18, 24, and 30 repeating units. From a three pulse photon echo shift measurement, they concluded that with increasing ring size, coupling to the bath weakened whereas intra-molecular coupling increased.

As the present study focuses on optical line shape, we first briefly discuss the pioneering work of Kubo.[40,41] This work of Kubo created the language we use in the discussion of line shapes. The analysis is general and was originally developed to explain nuclear magnetic resonance (NMR) line shape.[42–44]

Kubo's analysis starts with a simple stochastic equation of motion for the coordinate $x(t)$ of a harmonic oscillator coupled with its environment,

$$\dot{x}(t) = i\omega(t)\, x(t), \tag{1}$$

where x(t) is the harmonic oscillator co-ordinate and $\omega(t)$ is the frequency modulation by the interaction with environment. Time dependent frequency is expressed as

$$\omega(t) = \omega_0 + \delta\omega(t). \tag{2}$$

In Kubo formalism, the spectral line shape is defined as

$$I(\omega) = \frac{1}{2\pi}\int_{-\infty}^{\infty} e^{-i\omega t}\left\langle \exp\left(i\int_0^t \delta\omega(s)\, ds \right)\right\rangle dt, \tag{3}$$

where $\langle \ldots \rangle$ implies an averaging over a time trajectory, that is, a time average. When the frequency modulation is a Gaussian Markov stationary process, the cumulant beyond the second order vanishes. Since the time correlation function of the frequency modulation is exponential in time, the integral in the exponent can be carried out and the final expression is well-known and is given by

$$\phi(t) = \exp\left[-\Delta^2\tau_c^2 \left\{ \exp\left(-\frac{t}{\tau_c}\right) + \frac{t}{\tau_c} - 1 \right\} \right], \tag{4}$$

where Δ is the strength of the random modulation and τ_c is the relaxation time.

For slow modulation case, when τ_c is large, line shape is Gaussian and termed as inhomogenously broadened. For fast modulation case, time correlation function is exponential and line shape is Lorentzian which is often, as mentioned above, referred to as the motional narrowing limit. As the cumulant expansion beyond 2nd order vanishes, one may think that the above approach is correct but it may fail even for Gaussian bath, for the following reason. In the interaction representation (Eq. (7)), the full interaction is quantum mechanical and proper time ordering is required to truncate the cumulant expansion. Thus, even when the classical bath is Gaussian, the cumulant expansion may not be truncated trivially at the second order. The main point here is that the quantum stochastic Liouville equation (QSLE) does not suffer from such limitations and it can be implemented exactly for two state Poisson bath. The implementation of QSLE for Gaussian bath in principle can also be done exactly (as shown in Refs. 44 and 19). However its implementation is difficult, because one needs to include at least 6 or 7 excited bath states which make even a numerical approach prohibitively difficult. Nevertheless, QSLE provides an exact approach to the problem of quantum-classical mixed problems we encounter in spectroscopy.

It is straightforward to apply the QSLE-based Kubo line shape formalism even when we have multiple energy states participating in the dynamical process, such as in a dimer. However, the solution is now non-trivial. The reason is the increase of the number of fluctuation sources. For a dimer, we can now have two diagonal fluctuations and one off-diagonal fluctuation terms. In addition, there is usually a constant off-diagonal term in the dimer. The constant off-diagonal term gives rise to pronounced oscillations produced by quantum coherence between the two states.

As discussed by several authors, there are two well-known physical systems where coherence in population transfer dynamics could play important role. These are (i) thin films of conjugated polymers and (ii) photosynthetic reaction center. In both these systems, interplay between off-diagonal coupling J and fluctuation or dynamic disorder can limit the extent of coherence. Note that even in the absence of time dependent fluctuation, one can have static disorder in off-diagonal coupling. This could be particularly prevalent in thin films of conjugated polymer.

The initial theories of exciton transfer of Haken-Strobl-Reineker and that of Silbey *et al.* are based on the following standard (often referred to as Haken-Strobl) Hamiltonian:

$$H_{tot} = H_S + H_B + H_{\text{int}}, \tag{5}$$

where system (exciton) Hamiltonian is defined as a sum over lattice sites (running indices k and l)

$$H_S = \sum_k \omega_0 \left|k\right\rangle \left\langle k\right| + \sum_{\substack{k,l \\ k\neq l}} J_{kl} \left|k\right\rangle \left\langle l\right|. \tag{6}$$

Here ω_0 is the energy of an electronic exciton localized at site k and J_{kl} is the time independent off-diagonal interaction between excitations at sites k and l. H_B is the bath Hamiltonian and H_{int} is the interaction Hamiltonian between the system and the bath. We go over to the interaction representation of the bath to write the Hamiltonian as follows:

$$H(t) = H_S + V(t), \tag{7}$$

where, after setting $\hbar = 1$, $V(t)$ has the following form:

$$V\left(t\right) = e^{iH_B t} V_{class} e^{-iH_B t}. \tag{8}$$

Thus in the interaction representation of the bath, the coupling potential is time dependent which can be expressed as follows:

$$V(t) = \sum_k \left|k\right\rangle \left\langle k\right| V_d(t) + \sum_{\substack{k,l \\ k\neq l}} \left|k\right\rangle \left\langle l\right| V_{od}(t). \tag{9}$$

Here $V_d(t)$ denotes diagonal (local) and $V_{od}(t)$ represents off-diagonal (non-local) parts of the fluctuating potential V_{int}. As is customary in Kubo's stochastic Liouville equation, we model $V(t)$ by a stochastic function with known statistical properties. Using the above Hamiltonian, Bagchi and Oxtoby,[45] as well as Dutta and Bagchi[46] studied exciton diffusion in a one dimensional system of regularly placed two level systems, both in continuum and in discrete limits, respectively. We assume both the fluctuations to be described by Poisson stochastic process. In fact, the Poisson bath can be considered as a limiting form of Gaussian bath. In case of Poisson bath, diagonal and off-diagonal matrix elements jump between two values ($\pm V$) such that the average of each matrix element is zero. For most of the calculations reported here, we have, for simplicity, neglected the off-diagonal fluctuations. For real systems (photo-synthetic systems), off-diagonal fluctuations are often small compared to the diagonal one. However, we have considered an interesting role of off-diagonal fluctuations in exciton transport mechanism.

In this work, we are primarily interested in the study of quantum coherence that could be obtained from the optical line shapes in extended systems. In particular, we explore the correlation between optical line shape and quantum coherence in extended systems composed of equally spaced two levels. We also consider cyclic polymers composed of the correlated two level systems. We also briefly discuss the temperature effect and inclusion of vibrational mode in excitonic equation of motion which can be later used to study the real photosynthetic systems and conjugate polymers.

The main objectives of the present works are the following: (1) to study the line shape for excitation transfer in discrete model systems in slow and fast modulation limit, (2) to explore the effects of diagonal fluctuation for both correlated and uncorrelated bath case on the line shape for linear and cyclic systems, (3) to connect population transfer dynamics with line shape in both slow modulation and fast modulation limit for both linear and cyclic systems, and (4) to perform a detailed analysis of the propagation of coherence for correlated and uncorrelated bath case in slow and fast modulation limit.

In fast modulation limit, we obtain nearly the same results when all the baths are fully correlated (a limit we refer to as the correlated bath) as when they are completely uncorrelated. In this limit, both the line shape and the occupation probability function (OPF) are found to behave in a similar manner. However, in the slow modulation limit, the spatial correlation is found to be important. In the latter case, the line shapes as well as population transfer dynamics for the correlated bath and uncorrelated bath are significantly different. *We attribute this to the effects of quantum coherence affecting the two limits differently*.

The organization of the rest of the paper is as follows: In Sec. II, we explain Kubo's quantum stochastic Liouville equation (QSLE). In Sec. III, we discuss eigenvalue and eigenvector of Toeplitz matrix to explain line shape behavior in fast modulation limit. In Sec. IV, we describe calculation of line shape function for monomer. In Sec. V, we elucidate line shape calculation for multichromophoric systems. In Sec. VI, we qualitatively explain the role of off-diagonal fluctuation on line shape. In Sec. VII, we illustrate occupation probability function using QSLE. In Sec. VIII, we explore the propagation of coherence for correlated and uncorrelated bath case (diagonal fluctuation). In Sec. IX, we discuss the limitation of QSLE and effect of temperature on line shape and exciton transfer dynamics. In Sec. X, we discuss the temperature dependent equation of motion and the effect of vibrational mode on the exciton transfer dynamics. Finally, in Sec. XI, we draw the conclusion. Coupled equation of motion for dimer system in case of correlated bath can be found in Appendix A. Derivation coupled equation of motion for linear tetramer for uncorrelated bath case is provided in Appendix B.

II. QUANTUM STOCHASTIC LIOUVILLE EQUATION

Quantum stochastic Liouville equation (QSLE) was derived by Kubo to incorporate stochastic fluctuations in quantum Liouville equation. QSLE is ideally suited to describe dynamics of a quantum system interacting with a classical bath. It is extensively applied to electron spin resonance (ESR)

and nuclear magnetic resonance (NMR) studies as well as vibrational relaxation (for both energy and phase).

There are several studies of such coupled quantum system-classical bath systems.[47–50] Skinner and co-workers[51,52] made a notable contribution in this area in the context spectroscopy. Hernandez and Voth[53] explored the role of classical mechanics in defining coherence in quantum system through the calculation of time correlation function. Bagchi and Oxtoby studied exciton transport in one dimensional lattice considering correlated bath and uncorrelated bath for continuum model using QSLE. It was shown in the latter work that population transfer dynamics is sensitive to the nature of bath fluctuations in the non-Markovian limit.

We start with the quantum Liouville equation,

$$\frac{\partial \rho}{\partial t} = -\frac{i}{\hbar}\left[H(t), \rho\right], \tag{10}$$

where the Hamiltonian is given by Eq. (7). The master equation for probability measure is provided as follows:

$$\frac{\partial W(\mathrm{V}, t)}{\partial t} = \Gamma_{\mathrm{V}} W(\mathrm{V}, t), \tag{11}$$

where V is the random energy variable representing diagonal and off-diagonal fluctuations, $W(\mathrm{V}, t)$ is the probability that the random variable has a value V at time t, and Γ_{V} is the stochastic diffusion operator. For Gaussian-Markov process, the stochastic diffusion operator is a Fokker-Planck operator. For a Poisson bath, the stochastic operator can be represented by a matrix, as described in Sec. IV.

Now a joint probability distribution $P(\rho,V,t)$ is defined as follows:

$$P(\rho, \mathrm{V}, t) = \langle \delta(\rho - \rho(t))\, \delta(\mathrm{V} - \mathrm{V}(t)) \rangle . \tag{12}$$

The joint probability distribution, as the name and notation both denote, gives the probability of finding the system and bath term in given states simultaneously at time t. The average is to be taken over both system and bath variables.

In the next step, one derives an equation of motion for the joint probability distribution. We shall forego the details as they have described in many places. For the present work, we define a reduced density matrix $\sigma(t)$ as,

$$\sigma(t) = \int d\rho\, \rho\, P(\rho, \mathrm{V}, t) . \tag{13}$$

The integration is an averaging over the system variable to obtain the bath dependent dynamics.

Kubo showed that the reduced density matrix follows the following modified, stochastic quantum Liouville equation:

$$\frac{\partial \sigma}{\partial t} = -\frac{i}{\hbar}\left[H(t), \sigma\right] + \Gamma_{\mathrm{v}} \sigma. \tag{14}$$

Eq. (14) is known as Kubo's stochastic Liouville equation. The above equation can be used to study the energy transfer dynamics of the system. A different form of the equation is used to obtain the line shape function.[44] In this study, we have considered both correlated and uncorrelated bath cases. For correlated bath case, all the diagonal and off-diagonal fluctuations are spatially correlated all the time. On the other hand, for uncorrelated bath case, all the diagonal and off-diagonal fluctuations are completely uncorrelated.

III. USEFUL PROPERTIES OF TRIDIAGONAL TOEPLITZ MATRIX: EIGENVALUES AND EIGENVECTORS TO ANALYZE NATURE OF THE LINE SHAPE IN FAST MODULATION LIMIT

The study of coherence in our extended system of an array of two levels becomes simplified considerably by the use of certain properties of matrix algebra. In the absence of any fluctuation in the off-diagonal and diagonal terms, our system Hamiltonian with constant off-diagonal coupling J is a tri-diagonal Toeplitz matrix[54–56] in the site representation for linear system. This leads to several non-trivial observations. First, we have an analytic closed form expression for the eigenvalues and eigenvectors of the system. If we denote the off-diagonal terms by J, then the tri-diagonal matrix is given by

$$\begin{pmatrix} \omega_0 & J & 0 & 0 & 0 & 0 & 0 & \ldots\ldots \\ J & \omega_0 & J & 0 & 0 & 0 & 0 & \ldots\ldots \\ 0 & J & \omega_0 & 0 & 0 & 0 & \ldots\ldots & \\ 0 & 0 & J & \omega_0 & J & 0 & 0 & 0 \ldots\ldots \\ & & & \ldots\ldots & & & & \\ & & & \ldots\ldots & J & \omega_0 & & \end{pmatrix}. \tag{15}$$

Another remarkable property of this tri-diagonal Toeplitz matrix is that all the tri-diagonal Toeplitz matrices have same eigenvectors.

Another important result is that when $N \to \infty$, i.e., for infinite number of sites, for both linear and cyclic models, *all the eigenvalues are bounded*. For both of the systems, maximum and minimum eigenvalues are $\omega_0 \pm 2J$. Consequently for infinite size system, we obtain a dense spectrum with large number of peaks.

In the fast modulation limit when the rate of fluctuation is high and amplitudes of diagonal and off-diagonal coupling constants are small, the unperturbed system Hamiltonian can be used to analyze the nature of the line shape, particularly the positions of the peaks of the spectrum. In this case, system Hamiltonian is a Toeplitz matrix. We note in passing that for cyclic models, the matrices are known as circulant. The eigenvalues of Toeplitz matrix for linear and cyclic models give positions of the line shape peaks. Square of the coefficients in each eigenstates is related to the intensity of each peak. For linear and cyclic models, the expressions of eigenvalue and coefficients which are required to obtain the eigenstates are provided as follows.

A. Linear models

Here the eigenvalues are given by[54,56]

$$E_j = \omega_0 + 2J \cos\frac{j\pi}{N+1} \text{ (eigenvalues)}, \tag{16}$$

$$C_{jk} = \left(\frac{2}{N+1}\right)^{1/2} \sin\frac{jk\pi}{N+1} \text{ (coefficients of eigenvectors)}, \tag{17}$$

where N is total number of site, j = 1,2,3,. . .,N, and also k = 1,2,3,. . .,N. Note the following important points. First, the eigenvalues are bounded between $\omega_0 + 2J$ and $\omega_0 - 2J$.

Therefore, in the large N limit, the eigenvalues almost form a continuum. This is an important result as it suggests that the spectrum can be broad in the large N limit but bounded between the two limits given above. Second, the eigenfunctions can be easily found in an analytical form, from Equation (17). Thus, for a trimer where the unperturbed basis sets are localized site functions, the expressions for the eigenstates are as follows:

$$\begin{aligned}\psi_1 &= 0.5\phi_1 + 0.71\phi_2 + 0.5\phi_3, \quad \text{with } E_1 = \omega_0 + J/\sqrt{2}\\ \psi_2 &= 0.71\phi_1 - 0.71\phi_3, \quad \text{with } E_2 = \omega_0\\ \psi_3 &= 0.5\phi_1 - 0.71\phi_2 + 0.5\phi_3, \quad \text{with } E_3 = \omega_0 - J/\sqrt{2}\end{aligned}, \tag{18}$$

where ψ_i denotes the ith eigenstate of the system with eigenvalue E_j, and ϕ_i denotes ith molecular states without any intersite coupling.

The eigenvalues give the positions of the absorption maxima in the motional narrowing limit. There can be additional maxima in the case of static modulation, as we show later. Coefficients of eigenvectors are related to the intensities of the peaks. For all linear systems with odd number of sites, the centered peak has large intensity than the others and for those consisting of an even number of sites, the two peaks in the center have same intensity which is greater than all other peaks. For cyclic system, the situation is different and rather interesting. Here the intensities of peaks at lower frequency are greater than those at higher frequency due to the degeneracy of states.

Since the eigenvectors of our Toeplitz matrix are fully known, we can easily write down expressions for the wave functions of larger systems.

B. Cyclic models

In this case also we have analytical expressions of eigenvalues and eigenvectors that are given by similar expressions,

$$E_j = \omega_0 + 2J\cos\frac{2\pi(j-1)}{N} \text{ (eigenvalues)} \tag{19}$$

$$C_{jk} = \frac{1}{\sqrt{N}}\exp\left[\frac{2\pi i(k-1)(j-1)}{N}\right] \text{ (Coefficients for eigenvectors)}, \tag{20}$$

where N is total number of site, j = 1,2,3,. . .,N, and also k = 1,2,3,. . .,N.

For infinite number of site eigenvalues attain the maximum.

The peak positions obtained from QSLE equation are exactly the same as the ones given above.

For cyclic trimer, the lowest eigenvalue corresponds to doubly degenerate state. All the eigenstates are provided as follows:

$$\begin{aligned}\psi_1 &= 0.58(\phi_1 + \phi_2 + \phi_3), \quad \text{with } E_1 = \omega_0 + 2J,\\ \psi_2 &= 0.82\phi_1 - 0.41\phi_2 - 0.41\phi_3\\ \psi_3 &= 0.82\phi_1 + 0.71\phi_2 - 0.71\phi_3\end{aligned}; \quad \text{with } E_1 = \omega_0 - 2J. \tag{21}$$

In this case, intensity of the first peak is greater than that of the last peak. Due to degeneracy, we obtain only two peaks.

Toeplitz matrices are quite useful to describe the peak positions of line shape or splitting of line shape. Knoester and co-workers[57] used eigenvalues and eigenvectors for tridiagonal matrix for linear systems. However in this work, we have used eigenvalues and eigenvectors for both linear and cyclic models and compared the prediction of peak positions (eigenvalues) with the line shape obtained from QSLE approach.

IV. CALCULATION OF LINE SHAPE FUNCTION: MONOMER

We first present a study of monomer with QSLE as this is not only the simplest system (as only the site energy is subjected to the fluctuating environment) but also it helps bringing certain important aspects about QSLE in focus, as discussed below. We note that this is the same system as the one studied by Kubo long time ago to initiate systematic study of line shape problems, as discussed in Sec. I. Kubo's treatment however was phenomenological while the treatment given below follows a more accurate alternative derivation (again by Kubo and discussed below). Here we start with the following generalized definition of the line shape function:[44]

$$I(\omega) = \frac{\mu^2}{\pi}\,\mathrm{Re}\,\langle 0|\,X(i\omega)\,|0\rangle, \tag{22}$$

where

$$\dot{X}(t) = iHX + \Gamma X. \tag{23}$$

Here, the whole quantity inside the bra and ket multiplied by the pre-factor is similar as Fourier transform of transition dipole moment-dipole moment correlation function.

In the case of the Poisson bath, one can write the stochastic bath operator Γ and the eigenvectors as follows:

$$\Gamma = \begin{pmatrix} -\frac{b}{2} & \frac{b}{2} \\ \frac{b}{2} & -\frac{b}{2}\end{pmatrix}; \quad |0\rangle = \begin{pmatrix}1\\1\end{pmatrix}; \quad \langle 0| = \begin{pmatrix}\frac{1}{2} & \frac{1}{2}\end{pmatrix}. \tag{24}$$

We consider the ground state energy as zero. Then the Hamiltonian consists of energy of the excited state and diagonal fluctuation due to interaction of system with bath. Line shape function is given as

$$I(\omega) = \frac{\mu^2}{\pi}\frac{b_d\left[V_d^2 + (\omega-\omega_0)^2\right]}{\left[V_d^2 + (\omega-\omega_0)^2\right]^2 + 4b_d^2(\omega-\omega_0)^2}. \tag{25}$$

Figure 1 shows the line shape for the monomer. In this case, ω is scaled by V_d^2/b_d. We have kept the ratio V_d^2/b_d fixed. In this case, the change in the nature of line shape is quite small as maximum intensity of the peak is $\sim\frac{b_d}{V_d^2}$ and we consider inverse of the same as a fixed number. If the ratio is not kept fixed, then in the high value limit of b_d, the line shape approaches Kubo's motional narrowing limit, that is, the line shape is a sharp Lorentzian. However, when b_d decreases, the line shape broadens with low peak value of intensity but it does not approach the Gaussian functional form predicted by Kubo in this limit. This is probably due to the following reasons. In Kubo's treatment, the classical bath is assumed to be Gaussian. As a result, cumulant expansion beyond 2nd

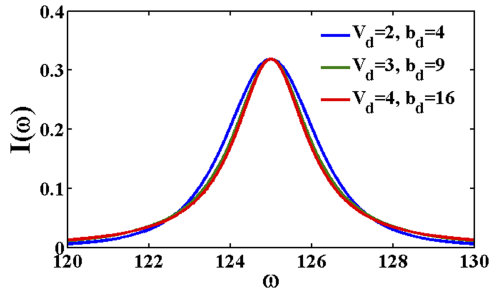

FIG. 1. Line shape function is plotted against frequency for different value of diagonal fluctuation strength and rate of fluctuation. Very small change in line shape behavior is observed as we fixed V_d^2/b_d ratio.

order is zero though the method is not fully correct (Sec. I). For Poisson bath case, all the cumulants exist and truncation after second order does not provide exact results. However, the approach we have used does not require such kind of approximation. The line shape for Poisson bath is exact for the chosen Hamiltonian. Note here that Kubo's simple line shape theory treats both static and fast modulation limit in terms of Δ and τ_c.

V. LINE SHAPE OF MULTICHROMOPHORIC SYSTEM

Here Kubo's[23] generalized line shape function can be written as

$$I(\omega) = \frac{1}{\pi} \mathrm{Re} \sum_{k,l} \mu_k \langle 0| X_{kl}(i\omega) |0\rangle \mu_l. \tag{26}$$

In this work, we assume that all the molecules are the same (all sites are equivalent) in all the models. Another important assumption is that the transition dipole moment couples to only one excitonic state. Hence from the definition of the line shape, only one transition dipole moment vector is required and the square of the transition dipole moment is the only constant quantity (other than the population density) that affects peak intensities.

If the transition dipole moments couple the ground state with only one excited state (say 1st excited state or excited state for site 1), we can write $\mu_1 \neq 0$ whereas all other elements are zero.

Subsequently Eq. (26) is reduced to the following expression:

$$I(\omega) = \frac{\mu_1^2}{\pi} \mathrm{Re} \langle 0| X_{11}(i\omega) |0\rangle, \tag{27}$$

where

$$\dot{X}(t) = iHX + \Gamma X. \tag{28}$$

X_{kl} is defined in the eigen basis. We have considered that all the molecules are identical and transition dipole moment only couples to one of the exciton states initially. For this reason, only the first component contributes to the line shape as given by Eq. (26). The assumption is not valid for many real cases.

We shall consider that the transition dipole moment as unity.

Laplace transform of Eq. (28) gives

$$(s - iH - \Gamma) X[s] = 1. \tag{29}$$

A. Dimer system

For a dimer, the Hamiltonian can be written generally as,

$$H = \begin{pmatrix} \omega_0 + V_d(t) & J + V_{od}(t) \\ J + V_{od}(t) & \omega_0 + V_d(t) \end{pmatrix}. \tag{30}$$

The diagonal and off-diagonal fluctuations can take only two values: $\pm V_d$ and $\pm V_{od}$. In the subsequent discussions in this section, we shall set off-diagonal fluctuation as zero. For real systems like the photosynthetic system, the value of off-diagonal fluctuations is quite low compared to the diagonal fluctuation and other parameters present in the Hamiltonian.

X_{kl} have two components and given as x_1 and x_2 for two excited states. We have used the Hamiltonian (Eq. (30)) which is a 2×2 matrix and we have substituted s by $i\omega$ in Eq. (29) to obtain Eq. (31). The basic space for Eq. (29) is 2×2 matrix. Hence it is convenient to write Eq. (29) in a general form as Eq. (31),

$$\begin{aligned} (s - i(\omega_0 + \mathbf{V_d}) - \mathbf{\Gamma}) \mathbf{x}_1 - iJ\mathbf{x}_2 &= \mathbf{x}_1^0 \\ (s - i(\omega_0 + \mathbf{V_d}) - \mathbf{\Gamma}) \mathbf{x}_1 - iJ\mathbf{x}_2 &= \mathbf{x}_2^0 \end{aligned}, \tag{31}$$

where $\mathbf{x}_1$ and $\mathbf{x}_2$ are the components of X, i.e., two different excited states of two molecules. For dimer systems, 3 states are possible when both the chromophores are in ground state and one is in excited or vice versa. As mentioned before, transition dipole moment only couples one of the excited states to the ground state. Solving Eq. (31) for $\mathbf{x}_1$ with the condition $\mathbf{x}_1^0 = 1$ and $\mathbf{x}_2^0 = 0$, we obtain the element $X_{11}[i\omega]$ in the form

$$X_{11}[i\omega] = (\mathbf{AA} - \mathbf{BB})^{-1}\mathbf{A}, \tag{32}$$

where

$$\mathbf{A} = \begin{pmatrix} i\omega - i\omega_0 - iV_d + \frac{b}{2} & -\frac{b}{2} \\ -\frac{b}{2} & i\omega - i\omega_0 + iV_d + \frac{b}{2} \end{pmatrix} \text{ and } \mathbf{B} = \begin{pmatrix} -iJ & 0 \\ 0 & -iJ \end{pmatrix}. \tag{33}$$

We now discuss the two limiting cases for bath fluctuations, one fully correlated and the other fully uncorrelated. For uncorrelated bath, Eq. (31) will be different as one has to consider all the fluctuations separately and invoke into Eq. (31).

1. Correlated bath

In case of the correlated bath, all the fluctuations are the same. Hence Eq. (32) can be used directly to obtain Eq. (34). For this case, we have used the definition of line shape, i.e., Eq. (27). Simple matrix operations (matrix multiplication, subtraction and inversion) are employed to obtain Eq. (34) from Eq. (32).

Hence the analytical expression for line shape function is given by

$$I = \frac{1}{2\pi}\,\mathrm{Re}\left[\frac{PQ^2 + PJ^2 + 2R^3 - 2PQR + 2J^2R - PR^2 - QR^2 + P^2Q + J^2Q}{(P^2 + J^2 + R^2)\,(Q^2 + J^2 + R^2) - (PR + RQ)^2}\right], \tag{34}$$

where

$$P = \left(i\omega - i\omega_0 - iV_d + \frac{b}{2}\right),\ Q = \left(i\omega - i\omega_0 + iV_d + \frac{b}{2}\right),\ R = -\frac{b_d}{2}. \tag{35}$$

For photosynthetic systems, spectroscopic measurements give $\omega_0 \sim 12\ 500\ \mathrm{cm}^{-1}$ and $J \sim 100$–$300\ \mathrm{cm}^{-1}$. Here we set $J = 1$; i.e., we scale all energy values by J. This gives $\omega_0 = 125$. Results are given in Figure 2.

2. Uncorrelated bath

Calculation of line shape of uncorrelated bath case is quite lengthy as one has to consider all the contribution from each of the uncorrelated bath. Hence both Eqs. (31) and (32) will be changed as one has to add all the contributions from all independent fluctuating terms and bath operators. We only provide plots of the line shape function in Figure 3.

B. Linear tetramer

Similarly for linear 4 site model, we can write Eq. (29) as follows:

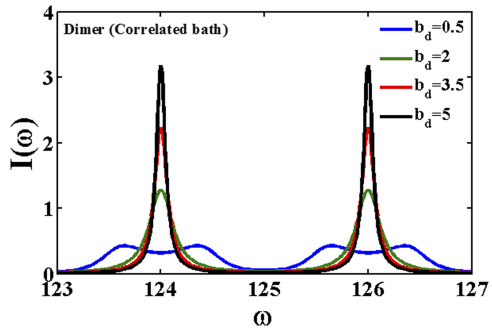

FIG. 2. Line shape function is plotted against frequency for dimer system at $J = 1$, $V_d = 0.5$ for correlated bath. Only b_d varies from low value to high value. Going from slow modulation to fast modulation limit, multiple peaks are merged with each other to show sharp and narrowed peaks.

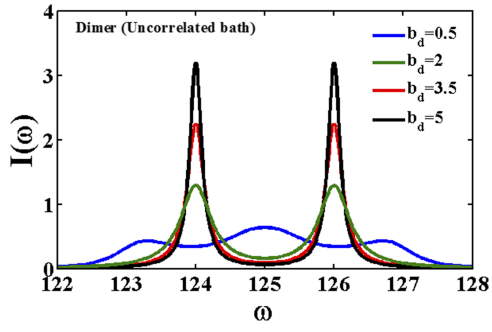

FIG. 3. Line shape function is plotted against frequency for dimer system at $J = 1$, $V_d = 0.5$ for uncorrelated bath. Only b_d varies from low value to high value. In slow modulation limit number of peaks are less than that of correlated bath case and peaks are broadened. In case of fast modulation limit intensity and broadening of all the peaks are greater than that of correlated bath case.

$$\begin{aligned}
\mathbf{A}\mathbf{x}_1 + \mathbf{B}\mathbf{x}_2 &= 1\\
\mathbf{B}\mathbf{x}_1 + \mathbf{A}\mathbf{x}_2 + \mathbf{B}\mathbf{x_3} &= 0\\
\mathbf{B}\mathbf{x}_2 + \mathbf{A}\mathbf{x}_3 + \mathbf{B}\mathbf{x_4} &= 0\\
\mathbf{B}\mathbf{x}_3 + \mathbf{A}\mathbf{x}_4 &= 0
\end{aligned}. \tag{36}$$

By solving the above Eq. (36), we get the expression of $X_{11}[i\omega]$ as follows:

$$\begin{aligned}
X_{11}[i\omega] = &\frac{1}{2}[(\mathbf{A}+\mathbf{B})\,\mathbf{A} - \mathbf{B}\mathbf{B}]^{-1}(\mathbf{A}+\mathbf{B})\\
&+ \frac{1}{2}[(\mathbf{A}-\mathbf{B})\,\mathbf{A} - \mathbf{B}\mathbf{B}]^{-1}(\mathbf{A}-\mathbf{B}).
\end{aligned} \tag{37}$$

A and **B** are already given for the case of two site model.

1. Correlated bath

Results are given in Figure 4 where the approach to the motional narrowing limit is observed with increase in b_d.

2. Uncorrelated bath

The results are depicted in Figure 5.

C. Cyclic tetramer

Similarly for cyclic 4 site model, we can write Eq. (29) as follows:

$$\begin{aligned}
\mathbf{A}\mathbf{x}_1 + \mathbf{B}\mathbf{x}_2 + \mathbf{B}\mathbf{x}_4 &= 1\\
\mathbf{B}\mathbf{x}_1 + \mathbf{A}\mathbf{x}_2 + \mathbf{B}\mathbf{x}_3 &= 0\\
\mathbf{B}\mathbf{x}_2 + \mathbf{A}\mathbf{x}_3 + \mathbf{B}\mathbf{x}_4 &= 0\\
\mathbf{B}\mathbf{x}_1 + \mathbf{B}\mathbf{x}_3 + \mathbf{A}\mathbf{x}_4 &= 0
\end{aligned}. \tag{38}$$

By solving the above Eq. (38), we get the expression of $X_{11}[i\omega]$ as follows:

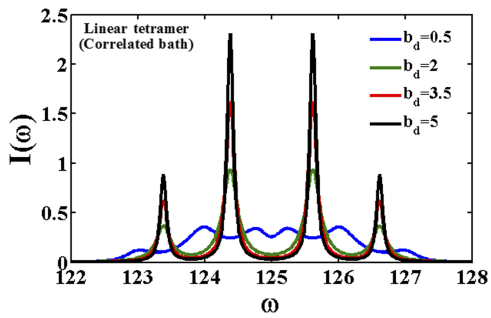

FIG. 4. Line shape function is plotted against frequency for linear tetramer system at $J = 1$, $V_d = 0.5$ for correlated bath. Only b_d varies from low value to high value. With increasing the rate of fluctuation, number of peaks decreases and all the peaks suggest motional narrowing behavior. Maximum intensity of the peaks is larger for dimer system than that of linear tetramer.

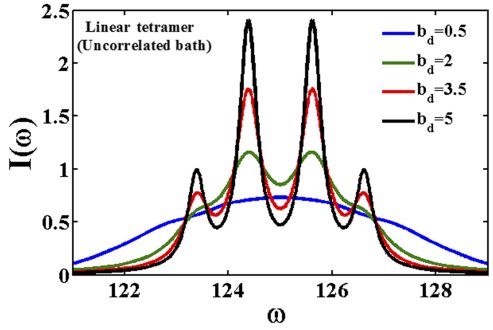

FIG. 5. Line shape function is plotted against frequency for linear tetramer system at $J = 1$, $V_d = 0.5$ for uncorrelated bath. Only b_d varies from low value to high value. In slow modulation limit, peaks are broadened and with increasing the modulation rate splitting of the peaks is taking place. Motional narrowing limit can be obtained by increasing b_d to a very large value (greater than that of uncorrelated bath case).

$$X_{11}[i\omega] = \frac{1}{2}[(\mathbf{A}+\mathbf{B})(\mathbf{A}+\mathbf{B}) - \mathbf{BB}]^{-1}(\mathbf{A}+\mathbf{B}) + \frac{1}{2}[(\mathbf{A}-\mathbf{B})(\mathbf{A}-\mathbf{B}) - \mathbf{BB}]^{-1}(\mathbf{A}-\mathbf{B}). \quad (39)$$

1. Correlated bath

The calculated results are given in Figure 6.

2. Uncorrelated bath

The calculated results are given in Figure 7.

We now briefly discuss the essential nature of Figures 2–7. In all of these figures, we have plotted the line shape for both correlated and uncorrelated bath for dimer, linear tetramer, and cyclic tetramer. For both the baths, the inter-site coupling J acts as an off-diagonal perturbation and is responsible for the splitting of the peaks. For linear system, the number of peaks is equal to the number of sites. For cyclic systems, the number of peaks is in accordance with the cyclic symmetry (that is, number of sites minus unity for cyclic tetramer). However, further splitting of the peak occurs with lowering the rate of fluctuation b_d. In the slow modulation limit of bath fluctuation, the stochastic perturbation can enhance coherence and give rise to new features. For all the models when b_d is quite low we have obtained multiple peaks and sometimes

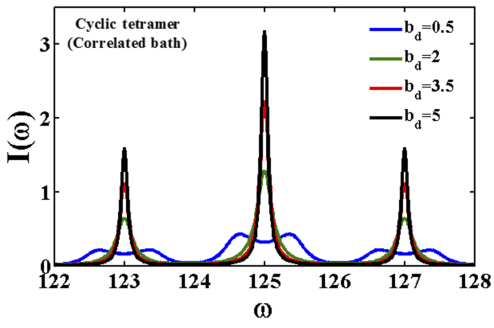

FIG. 6. Line shape function is plotted against frequency for cyclic tetramer system at $J = 1$, $V_d = 0.5$ for correlated bath. Only b_d varies from low value to high value. When we go from slow modulation to fast modulation limit, each pair of peaks merges with the other to produce a single peak. Maximum intensity of peaks for cyclic system is greater than that of linear system with same number of sites.

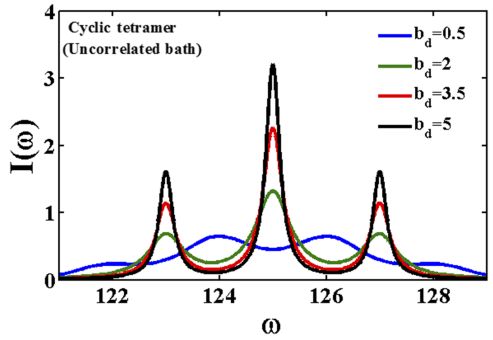

FIG. 7. Line shape function is plotted against frequency for cyclic tetramer system at $J = 1$, $V_d = 0.5$ for uncorrelated bath. Only b_d varies from low value to high value. In slow modulation limit peaks are broadened and with increasing the rate of fluctuation, intensity of peaks increases and shows the narrowing behavior.

the number of peaks is more than the number of sites present in the model. With increase in b_d, the stochastic perturbation vanishes and only the splitting due to the inter-site coupling survives. Also with increase in the rate of fluctuation, each of the peaks becomes sharp and their intensity increases. This limit is known as motional narrowing limit. For uncorrelated bath case, line shapes are broadened than that of correlated bath case. However, with increase in the number of sites, the broadening increases for uncorrelated bath case. The reason is as follows, with increase in number of sites, the number of uncorrelated baths increases which effectively destroys the mixing of the states. Another important feature is that with increase in number of sites for both linear and cyclic models, the intensity of the line shape decreases because of the fact that with increase in number of sites the delocalization of exciton as well as the coherence increases. The above site dependent study supports the observation of Donehue *et al.*[39] where they have observed with increase in ring size system-bath coupling gets weaker and intra-molecular coupling increases. When b_d is very high, i.e., in case of extreme motional narrowing limit, line shapes for both correlated and uncorrelated bath show similar behavior. However, the difference between correlated and uncorrelated bath increases with increase in the number of sites.

VI. EFFECT OF OFF-DIAGONAL FLUCTUATIONS ON LINE SHAPE

As highlighted earlier, in natural photosynthetic complex, the off-diagonal fluctuation is negligibly small compared to the diagonal fluctuation. We have also studied the effect of off-diagonal fluctuations in line shape though the results are not shown. Small amount of off-diagonal fluctuation breaks the symmetry of the peaks, i.e., the peak position shifts. However, with increase in the off-diagonal fluctuation, all the peaks merge with each other. Because of the off-diagonal fluctuations, inter-site coupling, i.e., J fluctuates which is responsible for the mixing of the states. As a result, splitting of the peaks ensues. In real systems, where all the fluctuations are present the line shapes are not symmetric. Scholes *et al.*[35,36] observed two peaks for dimer naphthalene; however, the line shape is not symmetric due to the vibrational contribution.

VII. OCCUPATION PROBABILITY FUNCTION (OPF) IN LINEAR AND CYCLIC POLYMERS

In our previous work,[46] we have studied occupation probability function (OPF) for linear polymer chain. Recently Fleming and Ishizaki,[14] Jang *et al.*,[8] Aspuru-Guzik *et al.*,[9,10] and Chen and Silbey[15] studied population relaxation dynamics in dimer and Fenna-Matthews-Olson (FMO) complex using different techniques. In this work, we have studied and compared the OPF of linear and cyclic tetramer.

As before, in this case also, we have investigated and compared correlated and uncorrelated bath cases. For the correlated bath case, all the diagonal and off-diagonal fluctuations are spatially correlated all the times. However, for uncorrelated bath case, fluctuations are uncorrelated, i.e., independent of each other at all the times. Correlated bath can also be called as same bath as all the sites are facing same environment always, whereas for uncorrelated bath case, all the sites are facing different environments all the time. They represent two extreme cases. In real systems, there must be a correlation length beyond which the bath fluctuations become uncorrelated. Correlated bath case may partly mimic exciton transport in the low temperature limit.

We have treated off-diagonal and diagonal fluctuation separately for uncorrelated bath case. For correlated bath case, coupled equation of motion can be written as

$$\frac{\partial \sigma_m}{\partial t} = -iH^x_{ex}\sigma_m - iV_d \sum_{m'=0}^{1} (\delta_{m+1,m'} + \delta_{m-1,m'}) \times \left(\sum_k |k\rangle\langle k| \right)^x \sigma_{m'} - iV_{od} \sum_{m'=0}^{1} (\delta_{m+1,m'} + \delta_{m-1,m'}) \times \left(\sum_{\substack{k,l \\ k\neq l}} |k\rangle\langle l| \right)^x \sigma_{m'} - mb\sigma_m, \tag{40}$$

where $O^x f = Of - fO$. For correlated bath case, population of each site is denoted as follows:

$$P_n(t) = \langle n|\, \sigma_0\, |n\rangle, \tag{41}$$

where n is the site number.

The QSLE for uncorrelated bath case can be written as

$$\frac{\partial \sigma}{\partial t} = -\frac{i}{\hbar}[H(t), \sigma] + \sum_j \Gamma_j \sigma, \tag{42}$$

where Γ_j is the stochastic force for jth random force.

For linear 4 sites model, four uncorrelated diagonal fluctuations are available. Hence one can write the coupled equation of motion for this system as follows (we have considered $\hbar = 1$) (details are provided in Appendix B):

$$\frac{\partial \sigma_{jmnp}}{\partial t} = -i\omega_0 \left(\sum_{k=1}^{4} |k\rangle\langle k| \right)^x \sigma_{jmnp} - iJ \left(\sum_{\substack{k=1,l=1 \\ k\neq l}}^{4} |k\rangle\langle l| \right)^x \sigma_{jmnp} - iV_d \sum_{j'=0}^{1} \left(\delta_{j+1,j'} + \delta_{j-1,j'} \right) (|1\rangle\langle 1|)^x \sigma_{j'mnp} - iV_d \sum_{m'=0}^{1} (\delta_{m+1,m'} + \delta_{m-1,m'}) (|2\rangle\langle 2|)^x \sigma_{jm'np} - iV_d \sum_{n'=0}^{1} (\delta_{n+1,n'} + \delta_{n-1,n'}) (|3\rangle\langle 3|)^x \sigma_{jmn'p} - iV_d \sum_{p'=0}^{1} \left(\delta_{p+1,p'} + \delta_{p-1,p'} \right) (|4\rangle\langle 4|)^x \sigma_{jmnp'} - jb_d\sigma_{jmnp} - mb_d\sigma_{jmnp} - nb_d\sigma_{jmnp} - pb_d\sigma_{jmnp}. \tag{43}$$

As stated before, V_d is the strength of the fluctuation. b_d denotes the rate of fluctuation. By symmetry, all the nearest neighbor independent diagonal fluctuations have same strength and also the same rate.

For uncorrelated bath with diagonal fluctuation, population of each site for linear system can be represented as follows:

$$P_n(t) = \langle n|\, \sigma_{\prod_{i=1}^{N} a_i}\, |n\rangle, \tag{44}$$

where n is the site number, N is the total number of site, and a_1,a_2,a_3,. . .,a_N all the elements are zero. In this work, we have considered a two state Poisson bath case which gives two eigenvalues: 0 and –b (see Appendix B). For the case with 0 eigenvalue, a_1,a_2,a_3,. . .,a_N elements are denoted with zero and while the other with –b eigenvalue, a_1,a_2,a_3,. . .,a_N elements are denoted by one.

For the cyclic 4 sites model, four uncorrelated diagonal fluctuations are available. One can write the coupled equation of motion for this system using QSLE as elaborated before.

We have defined normalized occupation probability function (OPF) as follows:

$$C^P_n(t) = \frac{P_n(t) - P_n(\infty)}{P_n(0) - P_n(\infty)}, \tag{45}$$

where P_n is the population of nth site. For uncorrelated bath case with off-diagonal fluctuation, population is denoted as $P_n(t) = \langle n|\, \sigma_{\prod_{i=1}^{N-1} a_i}\, |n\rangle$ for linear model whereas for cyclic model population is denoted as $P_n(t) = \langle n|\, \sigma_{\prod_{i=1}^{N} a_i}\, |n\rangle$, where N is the total site number and a_1,a_2,a_3,. . .,a_N all the elements are zero. We have calculated OPF for uncorrelated bath case with off-diagonal fluctuation for both 4 sites linear and cyclic model.

For uncorrelated bath case with only off-diagonal fluctuations, population for 4 sites linear model can be denoted as $P_n(t) = \langle n|\sigma_{000}|n\rangle$ because three uncorrelated off-diagonal fluctuations are present. However, population for 4 sites cyclic

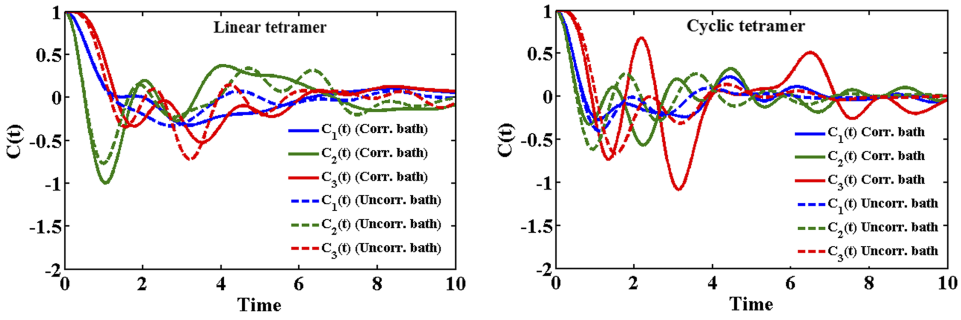

FIG. 8. Comparison plot of normalized occupation probability functions between the correlated and the uncorrelated bath (off-diagonal fluctuation) in slow modulation limit for (a) linear tetramer (b) cyclic tetramer at $J = 1$, $V_{od} = 0.5$, and $b_{od} = 0.5$. $\boldsymbol{C}_1(t)$, $\boldsymbol{C}_2(t)$, and $\boldsymbol{C}_3(t)$ are the normalized occupation probability function for site 1, site 2, and site 3, respectively. Solid line corresponds to correlated bath case and dashed line indicates uncorrelated bath case with off-diagonal fluctuation.

model can be designated as $P_n(t) = \langle n|\sigma_{0000}|n\rangle$ as four uncorrelated fluctuations are present in this case.

A. Comparison of occupation probability function (OPF) between correlated and uncorrelated bath case (off-diagonal fluctuation)

We have calculated the occupation probability function (OPF) for correlated and uncorrelated bath in slow and fast modulation limit. We have solved coupled equation of motion numerically using Runge-Kutta fourth order method. Dynamics of correlated bath does not involve diagonal fluctuation. Hence to compare the correlated and uncorrelated bath, we have calculated OPF for uncorrelated bath using only off-diagonal fluctuation. Change in OPF for uncorrelated bath (diagonal fluctuation) is quite small with increase in rate of fluctuation, i.e., going from slow to fast modulation limit because coherence cannot be directly destroyed by the diagonal fluctuation.

1. Slow modulation limit

The results are shown in Figure 8.

We have compared OPF between the correlated and the uncorrelated bath case (only off-diagonal fluctuation) in slow modulation limit ($J = 1$, $V_{od} = 0.5$, and $b_{od} = 0.5$) for linear and cyclic tetramer in Figure 8. For both linear and cyclic cases, correlated and uncorrelated bath OPFs show quite different behaviors. Similar observation is obtained for line shape in the slow modulation limit for both linear and cyclic models.

In the slow modulation limit, we have observed multiple peaks in the line shape and the number of observed peaks is greater than that can be surmised from the splitting of the energy levels and can be obtained from eigenvalues of Toeplitz matrix (only J acts as a perturbation). For correlated bath case, each of the peaks gets further splitted into two peaks which could only happen if the stochastic bath fluctuations themselves act as time independent multiple perturbations in addition with the inter-site coupling constant J. *This is an interesting outcome of this study*.

For the uncorrelated bath case, a similar pattern or behavior can be observed if we decrease the bath modulation rate. From occupation probability function, we also have observed different behavior for correlated and uncorrelated bath case. Oscillations are less for uncorrelated bath case because the large number of uncorrelated baths effectively destroys the coherence. The effect of stochastic bath fluctuation on coherence can be observed if one modulates the strength of the fluctuation with a fix modulation rate.

In the slow modulation limit case, if one decreases the value of the fluctuation strength, oscillation in occupation probability function increases which also suggests the increase of coherence. Also with decrease in fluctuation strength, number of peaks in line shape, i.e., splitting of the line shape also increases. In case of cyclic system, interference[58] between two possible path-ways increases the amplitude of oscillation in OPF.

2. Motional narrowing limit

The results are shown in Figure 9.

We have compared OPF between the correlated and the uncorrelated bath case with off-diagonal fluctuation in fast modulation limit for both linear and cyclic tetramer at $J = 1$, $V_{od} = 0.5$, and $b_{od} = 0.5$ in Figure 9. In the fast modulation limit (or the motional narrowing limit), oscillations in OPF for both linear and cyclic model occur with large amplitude. Both

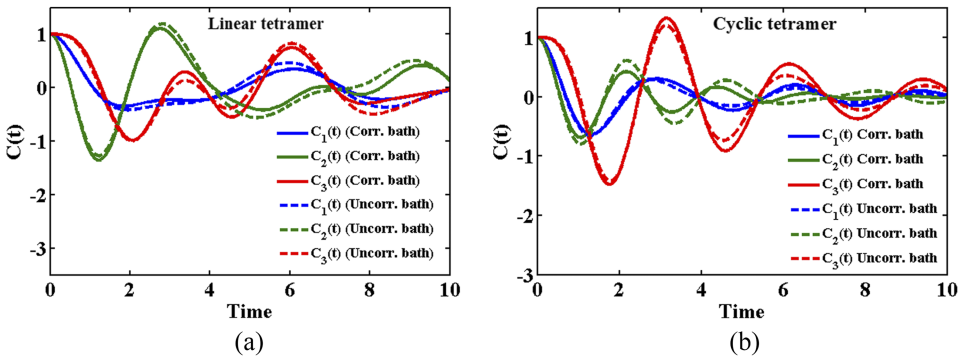

FIG. 9. Comparison plot of normalized occupation probability functions between the correlated and the uncorrelated bath (off-diagonal fluctuation) in fast modulation limit for (a) linear tetramer (b) cyclic tetramer at $J = 1$, $V_{od} = 0.5$, and $b_{od} = 5$. $\boldsymbol{C}_1(t)$, $\boldsymbol{C}_2(t)$, and $\boldsymbol{C}_3(t)$ are the normalized occupation probability function for site 1, site 2, and site 3, respectively. Solid line corresponds to correlated bath case and dashed line indicates uncorrelated bath case with off-diagonal fluctuation.

correlated and uncorrelated bath behave similarly in this limit. Like OPF, we also obtain similar line shape for correlated and uncorrelated bath and at a very high value of the rate of fluctuation (extreme motional narrowing limit) the agreement increases. In this limit, coherence survives in the system for a long time due to the inter-site coupling. Peak positions of the line shape coincide completely with the prediction obtained from the eigenvalue spectrum of Toeplitz matrix (only inter-site coupling J is involved). For high value of modulation rate, strength of the fluctuation has small role on coherence which is also clear from Eqs. (46) and (47) (given in Sec. VIII). Also the presence of interference effect between two possible ways of transfer shows sudden increase of oscillatory dynamics in the intermediate time regime for the cyclic system.

VIII. PROPAGATION OF QUANTUM COHERENCE

Propagation of coherence can be understood by studying the effects of the off-diagonal elements present in the coupled equation of motion for both correlated and uncorrelated bath cases. In this work, we have studied off-diagonal elements in equilibrium and excited bath modes for dimer system to examine which one dominates in slow and fast modulation limits, and also to explore the role of the rate of fluctuation (either b_d or b_{od}) in the propagation of coherence. According to the eigenvalue spectrum of the diffusion operator (Appendix B) for Poisson bath, two states are available (0 and –b). The states associated with 0 eigenvalue are the equilibrium bath mode and the states with –b eigenvalue are the excited bath mode.

A. Correlated bath case

Fortunately, we can solve the coupled equations of motion of exciton transfer dynamics (equations are provided in the Appendix A) analytically for a dimer system. We assume that initially there is no coherence and that the exciton is initially placed at site 1. We have also solved the population relaxation of each site in both slow modulation and fast modulation limit for larger system. The expressions for off-diagonal elements are provided as follows:

$$\langle 2|\sigma_0|1\rangle = i \sin 2Jt \exp\left(-\frac{b_{od}}{2}t\right)\left[\frac{b_{od}}{2a}\sinh\frac{a}{2}t + \frac{1}{2}\cosh\frac{a}{2}t\right], \tag{46}$$

$$\langle 2|\sigma_1|1\rangle = \frac{2iV_{od}}{a}\cos 2Jt \exp\left(-\frac{b_{od}}{2}t\right)\sinh\frac{a}{2}t, \tag{47}$$

where $a = \sqrt{b_{od}^2 - 16V_{od}^2}$.

To study the coherence, we provide plots of off-diagonal elements, i.e., coherence in equilibrium and excited bath state for both slow modulation and fast modulation limits (Figure 10).

All the elements plotted above are imaginary in nature. This can be understood from Eqs. (A1) and (A3). As population of each site is real, off-diagonal elements in equilibrium and excited bath modes have to be imaginary. In slow modulation limit described here, both the decays of $\langle 2|\sigma_0|1\rangle$ and $\langle 2|\sigma_1|1\rangle$ occur with the same rate. In fast modulation limit or motional narrowing limit, $\langle 2|\sigma_1|1\rangle$ decays more rapidly than that of $\langle 2|\sigma_0|1\rangle$. Hence one can conclude that for correlated bath case, in slow modulation limit, both the decays of equilibrium and excited bath modes occur in similar time. However, in motional narrowing limit, the excited bath modes decay more rapidly than that of the equilibrium bath modes.

B. Uncorrelated bath case (diagonal fluctuation)

In the case of uncorrelated bath, the total number of coupled equation of motion is large and we only provide plots of off-diagonal elements in both slow modulation and fast modulation limits, in Figure 11.

It is interesting to note that unlike the correlated bath case, for uncorrelated bath case in both slow modulation limit and motional narrowing limit, off-diagonal elements in equilibrium bath mode dominate over the off-diagonal element in the excited bath modes. In slow modulation limit, the decay of the off-diagonal element in both bath modes occurs in the same rate. However, in the motional narrowing limit, the decay of the off-diagonal element is so rapid that it is time invariant (that is, decay has been complete) over the relevant time range although the decay time of off-diagonal element in equilibrium bath modes does not change.

Hence from both correlated and uncorrelated bath cases, one can conclude that in slow modulation limit, both off-diagonal element in equilibrium and excited bath modes are responsible for the oscillation of OPF. However, in motional narrowing limit, the contribution in oscillatory OPF arises solely due to the off-diagonal element in equilibrium bath modes.

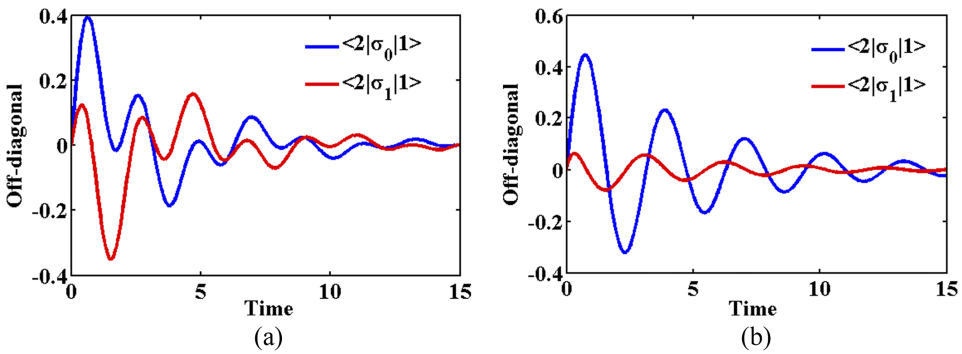

FIG. 10. Off-diagonal elements are plotted for the dimer problem against time for correlated bath case. (a) Propagation of off-diagonal elements in equilibrium and excited bath modes respectively in slow modulation limit at $J = 1$, $V_{od} = 0.5$, and $b_{od} = 0.5$. (b) Propagation of off-diagonal elements in equilibrium and excited bath modes, respectively, in the fast modulation limit at $J = 1$, $V_{od} = 0.5$, and $b_{od} = 5$.

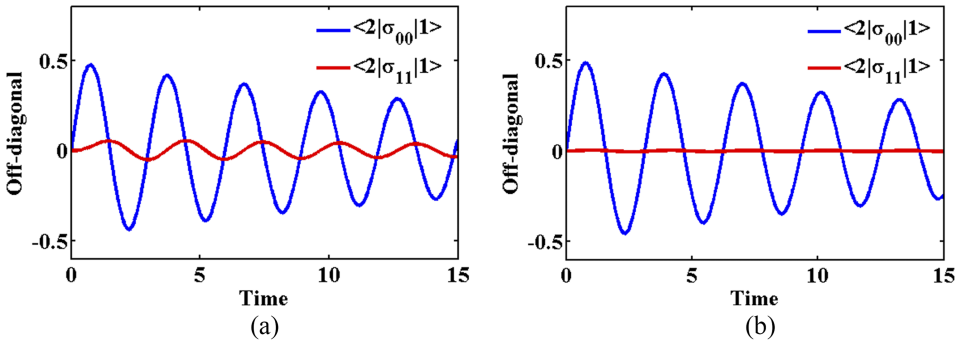

FIG. 11. Off-diagonal elements are plotted against time for the dimer problem for uncorrelated bath case (off-diagonal fluctuation) (a) imaginary part of $\langle 2|\boldsymbol{\sigma}_{00}|1\rangle$ and imaginary part of $\langle 2|\boldsymbol{\sigma}_{11}|1\rangle$ in slow modulation limit at $J = 1$, $V_{od} = 0.5$, and $b_{od} = 0.5$. (b) Imaginary part of $\langle 2|\boldsymbol{\sigma}_{00}|1\rangle$ and imaginary part of $\langle 2|\boldsymbol{\sigma}_{11}|1\rangle$ in fast modulation limit at $J = 1$, $V_{od} = 0.5$, and $b_{od} = 5$.

IX. EFFECT OF TEMPERATURE ON LINE SHAPE AND ENERGY TRANSFER DYNAMICS

One of the major limitations of quantum stochastic Liouville equation is that it cannot accurately account for the temperature effects in the line shape and energy transfer dynamics. This is because it cannot account for Boltzmann energy distribution in the population distribution. The temperature correction terms in QSLE were included by Kubo and Tanimura.[59,60]

A part of the temperature effects can be included through the amplitude (V) and rate (b) of diagonal and off-diagonal fluctuations. These effects are well-known and well-studied and need not be discussed. We just mention that J can have weaker temperature dependence than that of the terms V and b. With increasing temperature, diagonal fluctuations may increase rapidly, giving rise to broader line shape and maximum intensity of all the peaks becomes lower.

On the other hand, energy transfer dynamics may exhibit strong temperature dependence. At low temperature, fluctuations are slow and this could give rise to long lived coherences and lead to coherent energy transfer. With increase in temperature when rate of fluctuations increases, one can expect a crossover to incoherent dynamics and energy transfer may occur through incoherent hopping mechanism.

X. TEMPERATURE CORRECTION OF QUANTUM STOCHASTIC LIOUVILLE EQUATION AND INCLUSION OF VIBRATIONAL MODES

In this section, we briefly discuss the effect of temperature and vibrational mode in exciton transfer dynamics and analogous correction to QSLE equation as well as qualitative analysis in presence of both.

A. Temperature correction of QSLE equation

Effect of temperature is a highly non-trivial thing in quantum systems. The stochastic theory involves the fluctuation of energy states but does not include damping or dissipation term. Dissipation arises in addition to fluctuation because of the interaction of system with heat bath. In equilibrium energy balance occurs with the fluctuation-dissipation. The dissipation term does not appear in the stochastic Liouville equation as it ignores energy transfer from the system to the bath. Hence at finite temperature, system does not attain equilibrium at long time limit. Throughout the work, we neglected the effect of temperature. Here we first discuss the temperature correction of stochastic Liouville equation.[59,60] Then we include vibrational mode in that equation.

Tanimura and Kubo have considered bath as a collection of harmonic oscillators which leads to a Gaussian modulation of the system. They have used the Feynman–Vernon formalism to reduce the density matrix for system degrees of freedom. By assuming high-temperature and Markovian approximation as well as the Drude form of the spectral density of bath oscillators, they have obtained a set of equations of motion for the reduced density matrix. The main difference between these equations and the stochastic Liouville equation is that, in addition to the stochastic interaction term, it includes dissipation term which is missing in the stochastic model. These two terms are related through the fluctuation–dissipation theorem assuring the equilibrium state of the system at finite temperature at $t \to \infty$.

Temperature corrected stochastic Liouville equation for Gaussian modulation case can be written as follows:

$$\frac{\partial \sigma(\mathrm{V},t)}{\partial t} = \left[-iH(t)^x - b\frac{\partial}{\partial \mathrm{V}}\left(\mathrm{V} + \frac{\partial}{\partial \mathrm{V}}\right) - \frac{i\beta b}{2}\left(\mathrm{V} + \frac{\partial}{\partial \mathrm{V}}\right)V^o\right]\sigma(\mathrm{V},t), \tag{48}$$

where $H(t) = H^{ex} + V(t)$ and V is a random variable for the Gaussian modulation. First two terms on the right hand side of Eq. (48) are the same as the QSLE equation. Here $\beta = \frac{1}{k_B T}$, $O^o f = Of + fO$. The term associated with β is the reaction of the system to the bath and considered as a temperature correction term. This term leads the system to the thermal equilibrium.

We present the set of coupled equation of motion in hierarchy form using continued fractional approach as follows:

$$\frac{\partial \sigma_m}{\partial t} = -iH^x_{ex}\sigma_m - iV^x\sigma_{m+1} - i\left(V^x - \frac{\beta b}{2}V^o\right)\sigma_{m-1} - mb\sigma_m. \tag{49}$$

It is quite well known that truncation after second bath state (i.e., considering only 0 and 1) in QSLE equation provides the exact expression for Poisson bath or two state jump model. The coupled equation of motion for correlated bath case can be written as follows:

$$\frac{\partial \sigma_m}{\partial t} = -iH^x_{ex}\sigma_m - iV_d \sum_{m'=0}^{\infty} 2^{m'-m-1/2}(\delta_{m+1,m'} + 2m\delta_{m-1,m'}) \times \left(\sum_k |k\rangle\langle k|\right)^x \sigma_{m'}$$
$$- \frac{\beta V_d b_d}{2} \sum_{m'=0}^{\infty} 2^{m'-m-1/2} 2m\delta_{m-1,m'} \times \left(\sum_k |k\rangle\langle k|\right)^o \sigma_{m'} - iV_{od} \sum_{m'=0}^{\infty} 2^{m'-m-1/2}(\delta_{m+1,m'} + 2m\delta_{m-1,m'}) \times \left(\sum_{\substack{k,l \\ k\neq l}} |k\rangle\langle l|\right)^x \sigma_{m'}$$
$$- \frac{\beta V_{od} b_{od}}{2} \sum_{m'=0}^{\infty} 2^{m'-m-1/2} 2m\delta_{m-1,m'} \times \left(\sum_{\substack{k,l \\ k\neq l}} |k\rangle\langle l|\right)^o \sigma_{m'} - mb\sigma_m. \quad (50)$$

All the constant coefficients which depend upon the bath states are obtained from the expansion of reduced density matrix in the eigenfunction of bath.[45,58]

B. Effect of vibrational mode on exciton transfer dynamics

Temperature effect on the dynamics is large in presence of vibrational mode. Consequently one needs to incorporate the temperature effect and vibrational mode together to explain exciton transfer properly. In recent times, there have been several interesting studies[61,62] that consider the effect of vibrational mode on the exciton transfer dynamics.

If one considers the vibrational mode in the exciton transfer process, the above equation can be written as

$$\frac{\partial \sigma_m}{\partial t} = -iH^x_{ex}\sigma_m - iV_d \sum_{m'=0}^{1} 2^{m'-m-1/2}(\delta_{m+1,m'} + 2m\delta_{m-1,m'}) \times \left(\sum_{k,\nu} |k,\nu\rangle\langle k,\nu|\right)^x \sigma_{m'}$$
$$- \frac{\beta V_d b_d}{2} \sum_{m'=0}^{1} 2^{m'-m-1/2} 2m\delta_{m-1,m'} \times \left(\sum_k |k,\nu\rangle\langle k,\nu|\right)^o \sigma_{m'} - iV_{od} \sum_{m'=0}^{1} 2^{m'-m-1/2}(\delta_{m+1,m'} + 2m\delta_{m-1,m'})$$
$$\times \left(\sum_{\substack{k,l \\ k\neq l}} |k,\nu\rangle\langle l,\nu'|\right)^x \sigma_{m'} - \frac{\beta V_{od} b_{od}}{2} \sum_{m'=0}^{1} 2^{m'-m-1/2} 2m\delta_{m-1,m'} \times \left(\sum_{\substack{k,l \\ k\neq l}} |k,\nu\rangle\langle l,\nu'|\right)^o \sigma_{m'} - mb\sigma_m, \quad (51)$$

where

$$H^x_{ex} = \sum_{k,\nu} \left[\omega_k + \left(\nu + \frac{1}{2}\right)\varepsilon_0\right] (|k,\nu\rangle\langle k,\nu|)^x + \sum_{\substack{k,\nu,l,\nu' \\ k\neq l}} J_{k,\nu;l,\nu'} (|k,\nu\rangle\langle l,\nu'|)^x \quad (52)$$

and ε_0 is the vibrational zero point energy; ν and ν' are the vibrational quantum number.

Using these above equations, one can study the effect of vibrational mode on exciton transfer process. To study the dynamics, one needs to consider the vibronic transition. In this case, two coupling constants are important. For 0–0 vibronic transition, the coupling constant can be written as $J_{12}e^{-S/2}$. However for 0–1 vibronic transition, the coupling constant can be expressed as $-J_{12}\sqrt{S}e^{-S/2}$, where S is Huang-Rhys factor. Here one can assume that system-bath interaction terms or the fluctuation strength and rate of the fluctuation are independent of the state of the vibrational mode. For uncorrelated bath case, all the fluctuations are uncorrelated and one has to separately consider each fluctuating term (discussed in Sec. VII).

Here we discuss briefly the effect of vibrational mode on exciton transfer dynamics. In slow modulation limit when bath fluctuation is quite small, vibrational mode effects on large extent and oscillation decreases. Inclusion of vibrational mode adds new pathways for energy transfer and followed by the acceleration of the energy transfer dynamics. However in fast modulation limit when fluctuations are large, vibrational mode has very small effect in accelerating the dynamics, i.e., population dynamics more or less behave in similar manner in presence and absence of vibration. With increasing temperature, the contribution of vibrational mode to the dynamics of exciton transfer decreases. In future, we will study the effect of vibrational mode in energy transfer dynamics using temperature corrected equation of motion and the models will be appropriate to explain the exciton transfer in photosynthetic complex and conjugate polymer in a great detail.

XI. CONCLUSION

The present study investigates the nature of optical line shape in both linear chains and cyclic two level discrete model systems of different sizes, with both diagonal disorder and off-diagonal disorder, in both slow and fast modulation limits. We have studied the role of spatial correlations by considering two extreme models of bath space dependent correlation, termed as the correlated bath and the independent bath. Additionally, we have calculated population transfer dynamics in the same

systems in all the limits mentioned above. This allows us to interrogate signatures of coherence in the line shape.

Among various system sizes investigated, we have focused in this work on a (i) dimer, (ii) a linear chain of tetramer, and (iii) a cyclic tetramer. Many of the features observed are familiar from earlier line shape studies, such as a crossover from a static modulation to a motional narrowing limit with increase in the bath relaxation rate. There are, however, several new features arise from the extended nature of the system. Let us summarize the main results of the work.

(1) First and foremost, coherence in the extended systems of the type modeled here arises mostly from the presence of a constant inter-site coupling, denoted here by J. That is, the matrix element J needs to be non-zero. An interesting case arises when J is zero but off-diagonal coupling between sites is slowly varying and large. We discuss this point later.

(2) We have also discussed how one can analyze the nature of the line shape using property of Toeplitz matrix. In the absence of any fluctuations but with constant off-diagonal coupling J, the Hamiltonian of the system is a tridiagonal Toeplitz matrix. Now the eigenvalues of this matrix in our special case are exactly known. Therefore, we know exactly the peak positions of the line shape that we obtain in the fast modulation limit. This identity can be particularly useful because one can fit the peak positions to obtain the value of the off-diagonal coupling parameter J. Actually, this is the method used earlier to obtain the values of J from experimental line shape of a dimer. But to the best of our knowledge, this has not been implemented in such a detail earlier for larger chain or ring polymers.

(3) In the special and simple case of monomer, we observe a single sharp Lorentzian peak in the fast modulation limit (large b_d). With decrease in b_d, *the line shape broadens but one does not recover the Gaussian line shape in contrast to the prediction of Kubo's simple theory*. This suggests that Kubo's theory, based on cumulant expansion, may not be effective in the case of Poisson bath and for mixed quantum-classical systems. In the latter case, the bath statistics experienced by the system may be significantly non-Gaussian, as discussed long time ago by Oxtoby.[17]

(4) In the extreme slow modulation limit, *the system-bath coupling can act as an additional promoter of coherence between the sites and as a result the spacing between the peaks becomes larger than that given by J* via *Toeplitz matrix eigenvalues*. Interestingly, in limiting cases, the number of peaks can be greater than the total number of sites. In this interesting limit, a fewer peaks are observed for uncorrelated bath than that of correlated bath case, because the presence of large number of uncorrelated baths effectively destroys the mixing between the states. *Therefore, spatially correlated and uncorrelated baths show profoundly different behaviors in this limit*. Such effects are particularly important when the average off-diagonal coupling J is very small or zero but the fluctuating element (V_{od}) is large.

(5) In the fast modulation limit or the motional narrowing limit, coherence in the system due to the constant inter-site coupling (J) can be destroyed by fluctuations arising from bath degrees of freedom. Hence splitting of the peaks or number of the peaks for linear system follows the total number of sites and for cyclic system one can observe cyclic symmetry in the number of peaks. In this limit, both spatially correlated and uncorrelated baths show similar line shapes.

(6) In the slow modulation limit, correlated and uncorrelated bath cases exhibit profoundly different behaviors both in OPF and in line shape. In this limit, bath plays a crucial role to enhance the coherence and/or increase the oscillatory dynamics.

(7) In the fast modulation limit or motional narrowing limit, bath fluctuation reduces coherence and population transfer dynamics shows less oscillatory behavior. For both linear and cyclic models, we observe similar population transfer dynamics for correlated and uncorrelated baths. Also the intensities of the peaks are higher than that in the slow modulation case.

(8) We have investigated existence of coherence in a dimer system in the presence of both correlated and uncorrelated bath cases, in both slow and fast modulation limits. In the slow modulation limit for the correlated bath case, we have observed that the decay of off-diagonal elements in both equilibrium and excited bath modes occurs with the same rate. *However, in the fast modulation limit, off-diagonal element in the excited bath modes decays more rapidly than those in equilibrium bath mode*. The situation is somewhat different in the case of uncorrelated bath in slow modulation limit. Here the off-diagonal elements in the equilibrium bath mode dominate over the off-diagonal elements in the excited bath mode, although the decay occurs in same time. However, in motional narrowing limit, the decay of off-diagonal element in excited bath mode is so rapid that it remains essentially zero in the relevant time range where equilibrium mode decays.

(9) A well-known limitation of QSLE is its inability to relax the system to the Boltzmann energy distribution and hence its limitation in describing effects of temperature. With increasing temperature, diagonal fluctuations may increase rapidly consequently line shape becomes broad and maximum intensity of all the peaks decreases. For photosynthetic system, the site energy difference is comparable to thermal energy and hence temperature effect is quite significant. When temperature is low, exciton transport follows coherent dynamics. However, with increase in the temperature, transition from coherent to incoherent dynamics is expected. This can be similarly explained by the temperature dependence of all the parameters. Thus, QSLE can incorporate temperature effects indirectly through all the parameters used in this work.

We now discuss the relevance of our theoretical study to a few recent experimental observations. First, let us point out that the theory predicts that with increasing number of sites in the system, the intensity of each peak decreases in a certain definite

fashion (which is apparent from the Toeplitz matrix and which is proper to compare only within a particular type of model). This suggests that our theory can be used to explain, at this stage qualitatively, the experimental results of Donehue *et al.*[39] who have observed that with increasing the ring size, system-bath coupling weakens and intra-molecular coupling increases due to large delocalization of exciton in synthetic cyclic light harvesting pigment. In our study, we have also observed that with increase in ring size intensity decreases. In our model, this decrease happens due to the delocalization of the wave function that is the same as observed by Donehue *et al.* This can be interpreted as an increase of effective coupling between the sites and a decrease of system-bath interaction. This exchange narrowing effect is not new. In this study, we have highlighted how the line shape behavior changes with increasing the system size (site number). For this reason, we have compared the result with the observation of Donehue *et al.* They have investigated only for cyclic system. In our study for both cyclic and linear system we have observed with increasing system size the intensities of the line shapes decrease due to the increase in effective inter-site coupling. In this case with increasing system size, delocalization increases and line shapes become narrowed.

In several important studies, first Zewail *et al.* and subsequently Scholes *et al.*[35,36] observed splitting of the absorption band for dimer tetra-chloro benzene and dimer naphthalene, respectively. This can also be explained from the present theory as we also find, for the dimer system in the fast modulation limit, appearance of two well-separated peaks. As mentioned above, we can invoke the analytical result via Toeplitz matrix to obtain an estimate of coupling parameter J. We hope to address in a future work a detailed comparison between the theory developed here and the available experimental results. We have also explained the effect of temperature and vibrational mode in the excitionic equation of motion which can be used in future to study the real photosynthetic system and conjugated polymer in a detailed manner.

The present study needs to be generalized in several different directions because models employed here are rather idealistic in the sense that Haken-Strobl-Reineker-Silbey Hamiltonian ignores static disorder that could be prevalent in real systems (like in conjugated polymers). First, it may be worthwhile to study the effects of static or quenched randomness in the energy of the two level systems on both the exciton migration process and the optical line shape. Second, the effect of static randomness in the static off-diagonal coupling J can be quite interesting to investigate. These problems may be studied partly by using random Toeplitz matrix which itself is a problem of much current interest. The static randomness in both diagonal and off-diagonal energies brings this problem close to that of Anderson localization. It will be worthwhile to study effects of dynamic disorder in these problems.

ACKNOWLEDGMENTS

We thank Dr. Rajib Biswas and Professor Akihito Ishizaki for several useful discussions. We also thank Saumyak Mukherjee, Sayantan Mondal, and Puja Banerjee for careful reading of the final manuscript. We acknowledge the Department of Science and Technology (DST, India) for partial support of this work. B. Bagchi thanks Sir J. C. Bose Fellowship for providing partial financial support.

APPENDIX A: COUPLED EQUATION OF MOTION FOR CORRELATED BATH CASE FOR DIMER SYSTEM

Here we provide the coupled equations of motion for correlated bath case given as follows:

$$\langle 1|\dot{\sigma}_0|1\rangle = iJ\langle 1|\sigma_0|2\rangle - iJ\langle 2|\sigma_0|1\rangle + iV_{od}\langle 1|\sigma_1|2\rangle - iV_{od}\langle 2|\sigma_1|1\rangle\,, \tag{A1}$$

$$\langle 1|\dot{\sigma}_1|1\rangle = iJ\langle 1|\sigma_1|2\rangle - iJ\langle 2|\sigma_1|1\rangle + iV_{od}\langle 1|\sigma_0|2\rangle - iV_{od}\langle 2|\sigma_0|1\rangle - b\langle 1|\sigma_1|1\rangle\,, \tag{A2}$$

$$\langle 2|\dot{\sigma}_0|2\rangle = -iJ\langle 1|\sigma_0|2\rangle + iJ\langle 2|\sigma_0|1\rangle - iV_{od}\langle 1|\sigma_1|2\rangle + iV_{od}\langle 2|\sigma_1|1\rangle\,, \tag{A3}$$

$$\langle 2|\dot{\sigma}_1|2\rangle = -iJ\langle 1|\sigma_1|2\rangle + iJ\langle 2|\sigma_1|1\rangle - iV_{od}\langle 1|\sigma_0|2\rangle + iV_{od}\langle 2|\sigma_0|1\rangle - b_{od}\langle 2|\sigma_1|2\rangle\,, \tag{A4}$$

$$\langle 1|\dot{\sigma}_0|2\rangle = -iJ\langle 2|\sigma_0|2\rangle + iJ\langle 1|\sigma_0|1\rangle - iV_{od}\langle 2|\sigma_1|2\rangle + iV_{od}\langle 1|\sigma_1|1\rangle\,, \tag{A5}$$

$$\langle 1|\dot{\sigma}_1|2\rangle = -iJ\langle 2|\sigma_1|2\rangle + iJ\langle 1|\sigma_1|1\rangle - iV_{od}\langle 2|\sigma_0|2\rangle + iV_{od}\langle 1|\sigma_0|1\rangle - b_{od}\langle 1|\sigma_1|2\rangle\,, \tag{A6}$$

$$\langle 2|\dot{\sigma}_0|1\rangle = iJ\langle 2|\sigma_0|2\rangle - iJ\langle 1|\sigma_0|1\rangle + iV_{od}\langle 2|\sigma_1|2\rangle - iV_{od}\langle 1|\sigma_1|1\rangle\,, \tag{A7}$$

$$\langle 2|\dot{\sigma}_1|1\rangle = iJ\langle 2|\sigma_1|2\rangle - iJ\langle 1|\sigma_1|1\rangle + iV_{od}\langle 2|\sigma_0|2\rangle - iV_{od}\langle 1|\sigma_0|1\rangle - b_{od}\langle 2|\sigma_1|1\rangle\,. \tag{A8}$$

APPENDIX B: DERIVATION OF COUPLED EQUATION OF MOTION FOR LINEAR TETRAMER WITH UNCORRELATED BATH AND DIAGONAL FLUCTUATION

We provide a glimpse of the steps to obtain Eq. (43) from Eq. (42). For linear 4 sites model QSLE can be written as follows (considering only diagonal fluctuation):

$$\frac{\partial\sigma}{\partial t} = -\frac{i}{\hbar}[H(t),\sigma] + \Gamma_1\sigma + \Gamma_2\sigma + \Gamma_3\sigma + \Gamma_4\sigma, \tag{B1}$$

where Γ_1, Γ_2,Γ_3, and Γ_4 are the stochastic diffusion operator for V_{11}, V_{22}, V_{33}, and V_{44} (four diagonal elements), respectively.

Next step is the expansion of the reduced density matrix in eigenfunctions of Γ_1, Γ_2, Γ_3, and Γ_4 as,

$$\sigma = \sum_{j,m,n,p} \sigma_{jmnp} \left|b_j^1\right\rangle \left|b_m^2\right\rangle \left|b_n^3\right\rangle \left|b_p^4\right\rangle, \tag{B2}$$

where $\left|b_j^1\right\rangle$, $\left|b_m^2\right\rangle$, $\left|b_n^3\right\rangle$, and $\left|b_p^4\right\rangle$ represent the jth bath state of the diffusion operator Γ_1, mth bath state of the diffusion operator Γ_2, nth bath state of the diffusion operator Γ_3, and pth bath state of the diffusion operator Γ_4, respectively.

Eigenvalue of the diffusion operator Γ_1 can be written as follows:

$$\Gamma_1 \left|b_j^1\right\rangle = E_j \left|b_j^1\right\rangle. \tag{B3}$$

Eigenvalue of the other diffusion operators can be defined in similar fashion.

Substituting Eq. (B2) and eigenvalue equations into Eq. (B1), we obtain (considering $\hbar = 1$)

$$\begin{aligned}\sum_{j,m,n,p} \frac{\partial \sigma_{jmnp}}{\partial t} |b_j\rangle |b_m\rangle |b_n\rangle |b_p\rangle = -iH^x_{tot} \sum_{j,m,n,p} \sigma_{jmnp} |b_j\rangle |b_m\rangle |b_n\rangle |b_p\rangle + \sum_{j,m,n,p} E_j \sigma_{jmnp} |b_j\rangle |b_m\rangle |b_n\rangle |b_p\rangle \\ + \sum_{j,m,n,p} E_m \sigma_{jmnp} |b_j\rangle |b_m\rangle |b_n\rangle |b_p\rangle + \sum_{j,m,n,p} E_n \sigma_{jmnp} |b_j\rangle |b_m\rangle |b_n\rangle |b_p\rangle \\ + \sum_{j,m,n,p} E_p \sigma_{jmnp} |b_j\rangle |b_m\rangle |b_n\rangle |b_p\rangle.\end{aligned} \tag{B4}$$

After that replacing the full Hamiltonian (Eqs. (7) and (9)) into Eq. (B4) and followed by the multiplication with $\langle b_{j'}| \langle b_{m'}| \langle b_{n'}| \langle b_{p'}|$, we obtain

$$\begin{aligned}\frac{\partial \sigma_{jmnp}}{\partial t} = -iH^x_s \sigma_{jmnp} - i \sum_{j'} \left\langle b_{j'}\right| V_{11}(t) \left|b_j\right\rangle \left(\sum_k |k\rangle \langle k|\right)^x \sigma_{j'mnp} - i \sum_{m'} \langle b_{m'}| V_{22}(t) |b_m\rangle \left(\sum_{\substack{k,l \\ k\neq l}} |k\rangle \langle l|\right)^x \sigma_{jm'np} \\ - i \sum_{n'} \langle b_{n'}| V_{33}(t) |b_n\rangle \left(\sum_{\substack{k,l \\ k\neq l}} |k\rangle \langle l|\right)^x \sigma_{jmn'p} - i \sum_{p'} \left\langle b_{p'}\right| V_{44}(t) \left|b_p\right\rangle \left(\sum_{\substack{k,l \\ k\neq l}} |k\rangle \langle l|\right)^x \sigma_{jmnp'} + E_j \sigma_{jmnp} \\ + E_m \sigma_{jmnp} + E_n \sigma_{jmnp} + E_p \sigma_{jmnp}.\end{aligned} \tag{B5}$$

For Poisson bath, Γ can be expressed as 2×2 matrix as follows:

$$\Gamma = \begin{pmatrix} -\frac{b}{2} & \frac{b}{2} \\ \frac{b}{2} & -\frac{b}{2} \end{pmatrix}. \tag{B6}$$

Eigenvalues of Γ are 0 and $-b$. All the diagonal fluctuations have the following matrix elements in the eigenfunctions of diffusion operator as follows:

$$\begin{aligned}&\langle b_i| V_d(t) |b_j\rangle = V_d, \quad \text{where } i \neq j, \\ &\langle b_i| V_d(t) |b_i\rangle = 0.\end{aligned} \tag{B7}$$

The above Eq. (B7) is true for all the diagonal elements. Now inserting the eigenvalues of diffusion operator and Eq. (B7) into Eq. (B5) we obtain Eq. (43).

[1] G. S. Engel, T. R. Calhoun, E. L. Read, T.-K. Ahn, T. Mančal, Y.-C. Cheng, R. E. Blankenship, and G. R. Fleming, Nature **446**, 782 (2007).
[2] T. R. Calhoun, N. S. Ginsberg, G. S. Schlau-Cohen, Y.-C. Cheng, M. Ballottari *et al.* J. Phys. Chem. B **113**, 16291 (2009).
[3] D. Hu, J. Yu, K. Wong, B. Bagchi, P. Rossky, and P. Barbara, Nature **405**, 1030 (2000).
[4] E. Collini and G. D. Scholes, Science **323**, 369 (2009); J. Phys. Chem. A **113**, 4223 (2009).
[5] S. Saini and B. Bagchi, Phys. Chem. Chem. Phys. **12**, 7427 (2010).
[6] F. Sterpone, R. Martinazzo, A. N. Panda, and I. Burghardt, Z. Phys. Chem. **225**, 541 (2011).
[7] O. R. Tozer and W. Barford, J. Chem. Phys. **143**, 084102 (2015).
[8] S. Jang, Y. C. Cheng, D. R. Reichman, and J. D. Eaves, J. Chem. Phys. **129**, 101104 (2008).
[9] M. Mohseni, P. Rebentrost, S. Lloyd, and A. Aspuru-Guzik, J. Chem. Phys. **129**, 174106 (2008).
[10] P. Rebentrost, M. Mohseni, I. Kassal, S. Lloyd, and A. Aspuru-Guzik, New J. Phys. **11**, 033003 (2009).
[11] J. Cao and R. J. Silbey, J. Phys. Chem. A **113**, 13285 (2009).
[12] J. Wu, F. Liu, Y. Shen, J. Cao, and R. J. Silbey, New J. Phys. **12**, 105012 (2010).
[13] J. Wu, F. Liu, J. Ma, R. J. Silbey, and J. Cao, J. Chem. Phys. **137**, 174111 (2012).
[14] A. Ishizaki and G. R. Fleming, J. Chem. Phys. **130**, 234110 (2009); **130**, 234111 (2009).
[15] X. Chen and R. J. Silbey, J. Chem. Phys. **132**, 204503 (2010); J. Phys. Chem. B **115**, 5499 (2011).
[16] J. M. Moix, M. Khasin, and J. Cao, New J. Phys. **15**, 085010 (2013).
[17] D. W. Oxtoby, Annu. Rev. Phys. Chem. **32**, 77 (1981).
[18] D. W. Oxtoby, Adv. Chem. Phys. **47**, 487 (1981).
[19] B. Bagchi and D. W. Oxtoby, J. Phys. Chem. **86**, 2197 (1982).
[20] D. W. Oxtoby, J. Phys. Chem. **87**, 3028 (1983).
[21] K. F. Freed and A. A. Villaeys, Chem. Phys. **39**, 51 (1979).
[22] R. Zwanzig, Acc. Chem. Res. **23**, 148 (1990).
[23] A. H. Zewail and C. B. Harris, Chem. Phys. Lett. **28**, 8 (1974).
[24] A. H. Zewail and C. B. Harris, Phys. Rev. B **11**, 935 (1975); **11** 952 (1975).
[25] A. H. Zewail, Chem. Phys. Lett. **33**, 46 (1975).
[26] M. D. Fayer and C. B. Harris, Chem. Phys. Lett. **25**, 149 (1974).

[27]M. D. Fayer and C. B. Harris, Phys. Rev. B **9**, 748 (1974); **10**, 1784 (1974).
[28]H. Haken and G. Strobl, Z. Phys. **262**, 135 (1973).
[29]H. Haken and P. Reineker, Z. Phys. **249**, 253 (1972).
[30]P. Reineker, Phys. Status Solidi B **70**, 189 (1975).
[31]R. Silbey, Annu. Rev. Phys. Chem. **27**, 203 (1976).
[32]D. Yarkony and R. Silbey, J. Chem. Phys. **65**, 1042 (1976).
[33]H. Sumi, J. Chem. Phys. **67**, 2943 (1977).
[34]B. Jackson and R. Silbey, J. Chem. Phys. **75**, 3293 (1981).
[35]G. D. Scholes, K. P. Ghiggino, A. M. Oliver, and M. N. Paddon-Row, J. Am. Chem. Soc. **115**, 4345 (1993).
[36]F. Fassioli, R. Dinshaw, P. C. Arpin, and G. D. Scholes, J. R. Soc., Interface **11**, 20130901 (2013).
[37]S. Jang, M. D. Newton, and R. J. Silbey, J. Chem. Phys. **118**, 9312 (2003); **118**, 9324 (2003).
[38]M. Schröder, U. Kleinekathöfer, and M. Schreiber, J. Chem. Phys. **124**, 084903 (2006).
[39]J. E. Donehue, O. P. Varnavski, R. Cemborski, M. Iyoda, and T. Goodson III, J. Am. Chem. Soc. **133**, 4819 (2011).
[40]R. Kubo, J. Math. Phys. **4**, 174 (1963).
[41]B. Bagchi, *Molecular Relaxation in Liquids* (Oxford University Press, New York, 2012).
[42]R. Kubo and K. Tomita, J. Phys. Soc. Jpn. **9**, 888 (1954).
[43]R. Kubo, J. Phys. Soc. Jpn. **9**, 935 (1954).
[44]R. Kubo, Adv. Chem. Phys. **15**, 101 (1969).
[45]B. Bagchi and D. W. Oxtoby, J. Chem. Phys. **79**, 6211 (1983).
[46]R. Dutta and B. Bagchi, J. Chem. Phys. **145**, 164907 (2016).
[47]D. K. Garrity and J. L. Skinner, J. Chem. Phys. **82**, 260 (1985).
[48]J. S. Bader and B. J. Berne, J. Chem. Phys. **100**, 8359 (1994).
[49]S. A. Egrov, K. F. Everitt and J. L. Skinner, J. Phys. Chem. A **103**, 9494 (1999).
[50]P. A. Egelstaff, Adv. Phys. **11**, 203 (1962).
[51]J. L. Skinner and K. Park, J. Phys. Chem. B **105**, 6716 (2001).
[52]C. P. Lawrence and J. L. Skinner, J. Chem. Phys. **117**, 8847 (2002).
[53]R. Hernandez and G. A. Voth, Chem. Phys. **233**, 243 (1998).
[54]W. F. Trench, "Banded symmetric Toeplitz matrices: Where linear algebra borrows from difference equations," in Trinity University Mathematics Seminar, 2009.
[55]E. H. Bareiss, Numer. Math. **13**, 404 (1969).
[56]I. N. Levine, *Quantum Chemistry* (Prentice Hall, New Jersey, 2000).
[57]S. M. Vlaming, V. A. Malyshev, and J. Knoester, J. Chem. Phys. **127**, 154719 (2007).
[58]B. Bagchi and D. W. Oxtoby, J. Chem. Phys. **77**, 1391 (1982).
[59]Y. Tanimura and R. Kubo, J. Phys. Soc. Jpn. **58**, 101 (1989).
[60]Y. Tanimura, J. Phys. Soc. Jpn. **75**, 082001 (2006).
[61]N. Christensson, H. F. Kauffmann, T. Pullerits, and T. Mančal, J. Phys. Chem. B **116**, 7449 (2012).
[62]Y. Fujihashi, G. R. Fleming, and A. Ishizaki, J. Chem. Phys. **142**, 212403 (2015).